

Observation of $D^+ \rightarrow f_0(500)e^+\nu_e$ and Improved Measurements of $D \rightarrow \rho e^+\nu_e$

M. Ablikim¹, M. N. Achasov^{10,d}, S. Ahmed¹⁵, M. Albrecht⁴, M. Alekseev^{55A,55C}, A. Amoroso^{55A,55C}, F. F. An¹, Q. An^{52,42}, Y. Bai⁴¹, O. Bakina²⁷, R. Baldini Ferroli^{23A}, Y. Ban³⁵, K. Begzsuren²⁵, D. W. Bennett²², J. V. Bennett⁵, N. Berger²⁶, M. Bertani^{23A}, D. Bettoni^{24A}, F. Bianchi^{55A,55C}, E. Boger^{27,b}, I. Boyko²⁷, R. A. Briere⁵, H. Cai⁵⁷, X. Cai^{1,42}, A. Calcaterra^{23A}, G. F. Cao^{1,46}, S. A. Cetin^{45B}, J. Chai^{55C}, J. F. Chang^{1,42}, W. L. Chang^{1,46}, G. Chelkov^{27,b,c}, G. Chen¹, H. S. Chen^{1,46}, J. C. Chen¹, M. L. Chen^{1,42}, P. L. Chen⁵³, S. J. Chen³³, X. R. Chen³⁰, Y. B. Chen^{1,42}, W. Cheng^{55C}, X. K. Chu³⁵, G. Cibinetto^{24A}, F. Cossio^{55C}, H. L. Dai^{1,42}, J. P. Dai^{37,h}, A. Dbeyssi¹⁵, D. Dedovich²⁷, Z. Y. Deng¹, A. Denig²⁶, I. Denysenko²⁷, M. Destefanis^{55A,55C}, F. De Mori^{55A,55C}, Y. Ding³¹, C. Dong³⁴, J. Dong^{1,42}, L. Y. Dong^{1,46}, M. Y. Dong^{1,42,46}, Z. L. Dou³³, S. X. Du⁶⁰, P. F. Duan¹, J. Fang^{1,42}, S. S. Fang^{1,46}, Y. Fang¹, R. Farinelli^{24A,24B}, L. Fava^{55B,55C}, S. Fegan²⁶, F. Feldbauer⁴, G. Felici^{23A}, C. Q. Feng^{52,42}, E. Fioravanti^{24A}, M. Fritsch⁴, C. D. Fu¹, Q. Gao¹, X. L. Gao^{52,42}, Y. Gao⁴⁴, Y. G. Gao⁶, Z. Gao^{52,42}, B. Garillon²⁶, I. Garzia^{24A}, A. Gilman⁴⁹, K. Goetzen¹¹, L. Gong³⁴, W. X. Gong^{1,42}, W. Gradl²⁶, M. Greco^{55A,55C}, L. M. Gu³³, M. H. Gu^{1,42}, Y. T. Gu¹³, A. Q. Guo¹, L. B. Guo³², R. P. Guo^{1,46}, Y. P. Guo²⁶, A. Guskov²⁷, Z. Haddadi²⁹, S. Han⁵⁷, X. Q. Hao¹⁶, F. A. Harris⁴⁷, K. L. He^{1,46}, X. Q. He⁵¹, F. H. Heinsius⁴, T. Held⁴, Y. K. Heng^{1,42,46}, Z. L. Hou¹, H. M. Hu^{1,46}, J. F. Hu^{37,h}, T. Hu^{1,42,46}, Y. Hu¹, G. S. Huang^{52,42}, J. S. Huang¹⁶, X. T. Huang³⁶, X. Z. Huang³³, Z. L. Huang³¹, T. Hussain⁵⁴, W. Ikegami Andersson⁵⁶, M. Irshad^{52,42}, Q. Ji¹, Q. P. Ji¹⁶, X. B. Ji^{1,46}, X. L. Ji^{1,42}, H. L. Jiang³⁶, X. S. Jiang^{1,42,46}, X. Y. Jiang³⁴, J. B. Jiao³⁶, Z. Jiao¹⁸, D. P. Jin^{1,42,46}, S. Jin³³, Y. Jin⁴⁸, T. Johansson⁵⁶, A. Julin⁴⁹, N. Kalantar-Nayestanaki²⁹, X. S. Kang³⁴, M. Kavatsyuk²⁹, B. C. Ke¹, I. K. Keshk⁴, T. Khan^{52,42}, A. Khoukaz⁵⁰, P. Kiese²⁶, R. Kiuchi¹, R. Kliemt¹¹, L. Koch²⁸, O. B. Kolcu^{45B,f}, B. Kopf⁴, M. Kornicer⁴⁷, M. Kuemmel⁴, M. Kuessner⁴, A. Kupsc⁵⁶, M. Kurth¹, W. Kühn²⁸, J. S. Lange²⁸, P. Larin¹⁵, L. Lavezzi^{55C}, S. Leiber⁴, H. Leithoff²⁶, C. Li⁵⁶, Cheng Li^{52,42}, D. M. Li⁶⁰, F. Li^{1,42}, F. Y. Li³⁵, G. Li¹, H. B. Li^{1,46}, H. J. Li^{1,46}, J. C. Li¹, J. W. Li⁴⁰, K. J. Li⁴³, Kang Li¹⁴, Ke Li¹, Lei Li³, P. L. Li^{52,42}, P. R. Li^{46,7}, Q. Y. Li³⁶, T. Li³⁶, W. D. Li^{1,46}, W. G. Li¹, X. L. Li³⁶, X. N. Li^{1,42}, X. Q. Li³⁴, Z. B. Li⁴³, H. Liang^{52,42}, Y. F. Liang³⁹, Y. T. Liang²⁸, G. R. Liao¹², L. Z. Liao^{1,46}, J. Libby²¹, C. X. Lin⁴³, D. X. Lin¹⁵, B. Liu^{37,h}, B. J. Liu¹, C. X. Liu¹, D. Liu^{52,42}, D. Y. Liu^{37,h}, F. H. Liu³⁸, Fang Liu¹, Feng Liu⁶, H. B. Liu¹³, H. L. Liu⁴¹, H. M. Liu^{1,46}, Huanhuan Liu¹, Huihui Liu¹⁷, J. B. Liu^{52,42}, J. Y. Liu^{1,46}, K. Y. Liu³¹, Ke Liu⁶, L. D. Liu³⁵, Q. Liu⁴⁶, S. B. Liu^{52,42}, X. Liu³⁰, Y. B. Liu³⁴, Z. A. Liu^{1,42,46}, Zhiqing Liu²⁶, Y. F. Long³⁵, X. C. Lou^{1,42,46}, H. J. Lu¹⁸, J. G. Lu^{1,42}, Y. Lu¹, Y. P. Lu^{1,42}, C. L. Luo³², M. X. Luo⁵⁹, T. Luo^{9,j}, X. L. Luo^{1,42}, S. Lusso^{55C}, X. R. Lyu⁴⁶, F. C. Ma³¹, H. L. Ma¹, L. L. Ma³⁶, M. M. Ma^{1,46}, Q. M. Ma¹, X. N. Ma³⁴, X. Y. Ma^{1,42}, Y. M. Ma³⁶, F. E. Maas¹⁵, M. Maggiora^{55A,55C}, S. Maldaner²⁶, Q. A. Malik⁵⁴, A. Mangoni^{23B}, Y. J. Mao³⁵, Z. P. Mao¹, S. Marcello^{55A,55C}, Z. X. Meng⁴⁸, J. G. Messchendorp²⁹, G. Mezzadri^{24B}, J. Min^{1,42}, T. J. Min³³, R. E. Mitchell²², X. H. Mo^{1,42,46}, Y. J. Mo⁶, C. Morales Morales¹⁵, N. Yu. Muchnoi^{10,d}, H. Muramatsu⁴⁹, A. Mustafa⁴, S. Nakhoul^{11,g}, Y. Nefedov²⁷, F. Nerling¹¹, I. B. Nikolaev^{10,d}, Z. Ning^{1,42}, S. Nisar⁸, S. L. Niu^{1,42}, X. Y. Niu^{1,46}, S. L. Olsen⁴⁶, Q. Ouyang^{1,42,46}, S. Pacetti^{23B}, Y. Pan^{52,42}, M. Papenbrock⁵⁶, P. Patteri^{23A}, M. Pelizaeus⁴, J. Pellegrino^{55A,55C}, H. P. Peng^{52,42}, Z. Y. Peng¹³, K. Peters^{11,g}, J. Pettersson⁵⁶, J. L. Ping³², R. G. Ping^{1,46}, A. Pitka⁴, R. Poling⁴⁹, V. Prasad^{52,42}, H. R. Qi², M. Qi³³, T. Y. Qi², S. Qian^{1,42}, C. F. Qiao⁴⁶, N. Qin⁵⁷, X. S. Qin⁴, Z. H. Qin^{1,42}, J. F. Qiu¹, S. Q. Qu³⁴, K. H. Rashid^{54,i}, C. F. Redmer²⁶, M. Richter⁴, M. Ripka²⁶, A. Rivetti^{55C}, M. Rolo^{55C}, G. Rong^{1,46}, Ch. Rosner¹⁵, A. Sarantsev^{27,e}, M. Savrié^{24B}, K. Schoenning⁵⁶, W. Shan¹⁹, X. Y. Shan^{52,42}, M. Shao^{52,42}, C. P. Shen², P. X. Shen³⁴, X. Y. Shen^{1,46}, H. Y. Sheng¹, X. Shi^{1,42}, J. J. Song³⁶, W. M. Song³⁶, X. Y. Song¹, S. Sosio^{55A,55C}, C. Sowa⁴, S. Spataro^{55A,55C}, F. F. Sui³⁶, G. X. Sun¹, J. F. Sun¹⁶, L. Sun⁵⁷, S. S. Sun^{1,46}, X. H. Sun¹, Y. J. Sun^{52,42}, Y. K. Sun^{52,42}, Y. Z. Sun¹, Z. J. Sun^{1,42}, Z. T. Sun¹, Y. T. Tan^{52,42}, C. J. Tang³⁹, G. Y. Tang¹, X. Tang¹, M. Tiemens²⁹, B. Tsednee²⁵, I. Uman^{45D}, B. Wang¹, B. L. Wang⁴⁶, C. W. Wang³³, D. Wang³⁵, D. Y. Wang³⁵, Dan Wang⁴⁶, H. H. Wang³⁶, K. Wang^{1,42}, L. L. Wang¹, L. S. Wang¹, M. Wang³⁶, Meng Wang^{1,46}, P. Wang¹, P. L. Wang¹, W. P. Wang^{52,42}, X. F. Wang¹, Y. Wang^{52,42}, Y. F. Wang^{1,42,46}, Z. Wang^{1,42}, Z. G. Wang^{1,42}, Z. Y. Wang¹, Zongyuan Wang^{1,46}, T. Weber⁴, D. H. Wei¹², P. Weidenkaff²⁶, S. P. Wen¹, U. Wiedner⁴, M. Wolke⁵⁶, L. H. Wu¹, L. J. Wu^{1,46}, Z. Wu^{1,42}, L. Xia^{52,42}, X. Xia³⁶, Y. Xia²⁰, D. Xiao¹, Y. J. Xiao^{1,46}, Z. J. Xiao³², Y. G. Xie^{1,42}, Y. H. Xie⁶, X. A. Xiong^{1,46}, Q. L. Xiu^{1,42}, G. F. Xu¹, J. J. Xu^{1,46}, L. Xu¹, Q. J. Xu¹⁴, X. P. Xu⁴⁰, F. Yan⁵³, L. Yan^{55A,55C}, W. B. Yan^{52,42}, W. C. Yan², Y. H. Yan²⁰, H. J. Yang^{37,h}, H. X. Yang¹, L. Yang⁵⁷, R. X. Yang^{52,42}, S. L. Yang^{1,46}, Y. H. Yang³³, Y. X. Yang¹², Yifan Yang^{1,46}, Z. Q. Yang²⁰, M. Ye^{1,42}, M. H. Ye⁷, J. H. Yin¹, Z. Y. You⁴³, B. X. Yu^{1,42,46}, C. X. Yu³⁴, J. S. Yu³⁰, J. S. Yu²⁰, C. Z. Yuan^{1,46}, Y. Yuan¹, A. Yuncu^{45B,a},

A. A. Zafar⁵⁴, Y. Zeng²⁰, B. X. Zhang¹, B. Y. Zhang^{1,42}, C. C. Zhang¹, D. H. Zhang¹, H. H. Zhang⁴³,
H. Y. Zhang^{1,42}, J. Zhang^{1,46}, J. L. Zhang⁵⁸, J. Q. Zhang⁴, J. W. Zhang^{1,42,46}, J. Y. Zhang¹, J. Z. Zhang^{1,46},
K. Zhang^{1,46}, L. Zhang⁴⁴, S. F. Zhang³³, T. J. Zhang^{37,b}, X. Y. Zhang³⁶, Y. Zhang^{52,42}, Y. H. Zhang^{1,42},
Y. T. Zhang^{52,42}, Yang Zhang¹, Yao Zhang¹, Yu Zhang⁴⁶, Z. H. Zhang⁶, Z. P. Zhang⁵², Z. Y. Zhang⁵⁷, G. Zhao¹,
J. W. Zhao^{1,42}, J. Y. Zhao^{1,46}, J. Z. Zhao^{1,42}, Lei Zhao^{52,42}, Ling Zhao¹, M. G. Zhao³⁴, Q. Zhao¹, S. J. Zhao⁶⁰,
T. C. Zhao¹, Y. B. Zhao^{1,42}, Z. G. Zhao^{52,42}, A. Zhemchugov^{27,b}, B. Zheng⁵³, J. P. Zheng^{1,42}, W. J. Zheng³⁶,
Y. H. Zheng⁴⁶, B. Zhong³², L. Zhou^{1,42}, Q. Zhou^{1,46}, X. Zhou⁵⁷, X. K. Zhou^{52,42}, X. R. Zhou^{52,42}, X. Y. Zhou¹,
Xiaoyu Zhou²⁰, Xu Zhou²⁰, A. N. Zhu^{1,46}, J. Zhu³⁴, J. Zhu⁴³, K. Zhu¹, K. J. Zhu^{1,42,46}, S. Zhu¹,
S. H. Zhu⁵¹, X. L. Zhu⁴⁴, Y. C. Zhu^{52,42}, Y. S. Zhu^{1,46}, Z. A. Zhu^{1,46}, J. Zhuang^{1,42}, B. S. Zou¹, J. H. Zou¹

(BESIII Collaboration)

¹ *Institute of High Energy Physics, Beijing 100049, People's Republic of China*

² *Beihang University, Beijing 100191, People's Republic of China*

³ *Beijing Institute of Petrochemical Technology, Beijing 102617, People's Republic of China*

⁴ *Bochum Ruhr-University, D-44780 Bochum, Germany*

⁵ *Carnegie Mellon University, Pittsburgh, Pennsylvania 15213, USA*

⁶ *Central China Normal University, Wuhan 430079, People's Republic of China*

⁷ *China Center of Advanced Science and Technology, Beijing 100190, People's Republic of China*

⁸ *COMSATS Institute of Information Technology, Lahore, Defence Road, Off Raiwind Road, 54000 Lahore, Pakistan*

⁹ *Fudan University, Shanghai 200443, People's Republic of China*

¹⁰ *G.I. Budker Institute of Nuclear Physics SB RAS (BINP), Novosibirsk 630090, Russia*

¹¹ *GSI Helmholtzcentre for Heavy Ion Research GmbH, D-64291 Darmstadt, Germany*

¹² *Guangxi Normal University, Guilin 541004, People's Republic of China*

¹³ *Guangxi University, Nanning 530004, People's Republic of China*

¹⁴ *Hangzhou Normal University, Hangzhou 310036, People's Republic of China*

¹⁵ *Helmholtz Institute Mainz, Johann-Joachim-Becher-Weg 45, D-55099 Mainz, Germany*

¹⁶ *Henan Normal University, Xinxiang 453007, People's Republic of China*

¹⁷ *Henan University of Science and Technology, Luoyang 471003, People's Republic of China*

¹⁸ *Huangshan College, Huangshan 245000, People's Republic of China*

¹⁹ *Hunan Normal University, Changsha 410081, People's Republic of China*

²⁰ *Hunan University, Changsha 410082, People's Republic of China*

²¹ *Indian Institute of Technology Madras, Chennai 600036, India*

²² *Indiana University, Bloomington, Indiana 47405, USA*

²³ *(A)INFN Laboratori Nazionali di Frascati, I-00044, Frascati,*

Italy; (B)INFN and University of Perugia, I-06100, Perugia, Italy

²⁴ *(A)INFN Sezione di Ferrara, I-44122, Ferrara, Italy; (B)University of Ferrara, I-44122, Ferrara, Italy*

²⁵ *Institute of Physics and Technology, Peace Ave. 54B, Ulaanbaatar 13330, Mongolia*

²⁶ *Johannes Gutenberg University of Mainz, Johann-Joachim-Becher-Weg 45, D-55099 Mainz, Germany*

²⁷ *Joint Institute for Nuclear Research, 141980 Dubna, Moscow region, Russia*

²⁸ *Justus-Liebig-Universitaet Giessen, II. Physikalisches Institut, Heinrich-Buff-Ring 16, D-35392 Giessen, Germany*

²⁹ *KVI-CART, University of Groningen, NL-9747 AA Groningen, Netherlands*

³⁰ *Lanzhou University, Lanzhou 730000, People's Republic of China*

³¹ *Liaoning University, Shenyang 110036, People's Republic of China*

³² *Nanjing Normal University, Nanjing 210023, People's Republic of China*

³³ *Nanjing University, Nanjing 210093, People's Republic of China*

³⁴ *Nankai University, Tianjin 300071, People's Republic of China*

³⁵ *Peking University, Beijing 100871, People's Republic of China*

³⁶ *Shandong University, Jinan 250100, People's Republic of China*

³⁷ *Shanghai Jiao Tong University, Shanghai 200240, People's Republic of China*

³⁸ *Shanxi University, Taiyuan 030006, People's Republic of China*

³⁹ *Sichuan University, Chengdu 610064, People's Republic of China*

⁴⁰ *Soochow University, Suzhou 215006, People's Republic of China*

- ⁴¹ Southeast University, Nanjing 211100, People's Republic of China
⁴² State Key Laboratory of Particle Detection and Electronics, Beijing 100049, Hefei 230026, People's Republic of China
⁴³ Sun Yat-Sen University, Guangzhou 510275, People's Republic of China
⁴⁴ Tsinghua University, Beijing 100084, People's Republic of China
⁴⁵ (A)Ankara University, 06100 Tandogan, Ankara, Turkey; (B)Istanbul Bilgi University, 34060 Eyup, Istanbul, Turkey; (C)Uludag University, 16059 Bursa, Turkey; (D)Near East University, Nicosia, North Cyprus, Mersin 10, Turkey
⁴⁶ University of Chinese Academy of Sciences, Beijing 100049, People's Republic of China
⁴⁷ University of Hawaii, Honolulu, Hawaii 96822, USA
⁴⁸ University of Jinan, Jinan 250022, People's Republic of China
⁴⁹ University of Minnesota, Minneapolis, Minnesota 55455, USA
⁵⁰ University of Muenster, Wilhelm-Klemm-Str. 9, 48149 Muenster, Germany
⁵¹ University of Science and Technology Liaoning, Anshan 114051, People's Republic of China
⁵² University of Science and Technology of China, Hefei 230026, People's Republic of China
⁵³ University of South China, Hengyang 421001, People's Republic of China
⁵⁴ University of the Punjab, Lahore-54590, Pakistan
⁵⁵ (A)University of Turin, I-10125, Turin, Italy; (B)University of Eastern Piedmont, I-15121, Alessandria, Italy; (C)INFN, I-10125, Turin, Italy
⁵⁶ Uppsala University, Box 516, SE-75120 Uppsala, Sweden
⁵⁷ Wuhan University, Wuhan 430072, People's Republic of China
⁵⁸ Xinyang Normal University, Xinyang 464000, People's Republic of China
⁵⁹ Zhejiang University, Hangzhou 310027, People's Republic of China
⁶⁰ Zhengzhou University, Zhengzhou 450001, People's Republic of China
- ^a Also at Bogazici University, 34342 Istanbul, Turkey
^b Also at the Moscow Institute of Physics and Technology, Moscow 141700, Russia
^c Also at the Functional Electronics Laboratory, Tomsk State University, Tomsk, 634050, Russia
^d Also at the Novosibirsk State University, Novosibirsk, 630090, Russia
^e Also at the NRC "Kurchatov Institute", PNPI, 188300, Gatchina, Russia
^f Also at Istanbul Arel University, 34295 Istanbul, Turkey
^g Also at Goethe University Frankfurt, 60323 Frankfurt am Main, Germany
^h Also at Key Laboratory for Particle Physics, Astrophysics and Cosmology, Ministry of Education; Shanghai Key Laboratory for Particle Physics and Cosmology; Institute of Nuclear and Particle Physics, Shanghai 200240, People's Republic of China
ⁱ Also at Government College Women University, Sialkot - 51310. Punjab, Pakistan.
^j Also at Key Laboratory of Nuclear Physics and Ion-beam Application (MOE) and Institute of Modern Physics, Fudan University, Shanghai 200443, People's Republic of China

(Dated: February 21, 2019)

Using a data sample corresponding to an integrated luminosity of 2.93 fb^{-1} recorded by the BESIII detector at a center-of-mass energy of 3.773 GeV, we present an analysis of the decays $D^0 \rightarrow \pi^- \pi^0 e^+ \nu_e$ and $D^+ \rightarrow \pi^- \pi^+ e^+ \nu_e$. By performing a partial wave analysis, the $\pi^+ \pi^-$ S -wave contribution to $D^+ \rightarrow \pi^- \pi^+ e^+ \nu_e$ is observed to be $(25.7 \pm 1.6 \pm 1.1)\%$ with a statistical significance greater than 10σ , besides the dominant P -wave contribution. This is the first observation of the S -wave contribution. We measure the branching fractions $\mathcal{B}(D^0 \rightarrow \rho^- e^+ \nu_e) = (1.445 \pm 0.058 \pm 0.039) \times 10^{-3}$, $\mathcal{B}(D^+ \rightarrow \rho^0 e^+ \nu_e) = (1.860 \pm 0.070 \pm 0.061) \times 10^{-3}$, and $\mathcal{B}(D^+ \rightarrow f_0(500) e^+ \nu_e, f_0(500) \rightarrow \pi^+ \pi^-) = (6.30 \pm 0.43 \pm 0.32) \times 10^{-4}$. An upper limit of $\mathcal{B}(D^+ \rightarrow f_0(980) e^+ \nu_e, f_0(980) \rightarrow \pi^+ \pi^-) < 2.8 \times 10^{-5}$ is set at the 90% confidence level. We also obtain the hadronic form factor ratios of $D \rightarrow \rho e^+ \nu_e$ at $q^2 = 0$ assuming the single-pole dominance parametrization: $r_V = \frac{V(0)}{A_1(0)} = 1.695 \pm 0.083 \pm 0.051$, $r_2 = \frac{A_2(0)}{A_1(0)} = 0.845 \pm 0.056 \pm 0.039$.

The nature of the light scalar mesons $f_0(500)$, $f_0(980)$, and $a_0(980)$ has been controversial for many years [1]. The investigation of their structure can improve our understanding of the chiral-symmetry-breaking mechanisms of quantum chromodynamics (QCD) and quark confinement physics. A $q\bar{q}$ configuration in the naive quark model cannot explain their mass ordering, while there is still the possibility of being mixtures of $q\bar{q}$ states. The other interpretations are often diquark-antidiquark states (tetraquark) [2] and meson-meson bound states [3]. The difficulty in unraveling this question has been due to the simultaneous presence of several different sources of non-perturbative strong interactions.

Since the leptons and hadrons in the final state interact with each other only weakly, the semileptonic (SL) decay of $D^+ \rightarrow f_0(500)e^+\nu_e$ provides a unique and clean platform. A sizable branching fraction (BF) of this decay is predicted by some theoretical models [4, 5]. In addition, the P -wave dominance of the $\pi\pi$ system in this decay could be utilized to measure the hadronic form factor (FF), which can in turn check theoretical approaches such as lattice QCD [6] and QCD sum rules [7].

In the previous study at the CLEO-c experiment [8], no significant indication for the S wave was seen. In this Letter, by performing a partial wave analysis (PWA) of $D^0 \rightarrow \pi^-\pi^0e^+\nu_e$ and $D^+ \rightarrow \pi^-\pi^+e^+\nu_e$, we report the first observation of $D^+ \rightarrow f_0(500)e^+\nu_e$, the measurements of the FF ratios for $D \rightarrow \rho e^+\nu_e$, and the related BFs. For the BF measurement of SL decay, we use the double-tag technique [9]. Charge conjugate states are implied throughout this Letter. The analysis is performed based on a data sample corresponding to an integrated luminosity of 2.93 fb^{-1} [10, 11] collected with the BESIII detector in e^+e^- annihilation at a center-of-mass energy (\sqrt{s}) of 3.773 GeV. The BESIII detector is described in detail elsewhere [12].

The generic Monte Carlo (MC) sample, described in Ref. [13], has been verified to its validity to simulate the background in this analysis. The signal MC sample consists of exclusive decays $\psi(3770) \rightarrow D\bar{D}$, where the D decays to the SL signal modes, with the decay-product distribution determined by the results of our PWA, while the \bar{D} decays inclusively, as in the generic MC sample.

A detailed description of the selection criteria for charged and neutral particle candidates is provided in Ref. [13]. The tagged \bar{D} mesons are reconstructed by appropriate combinations of the charged tracks and π^0 candidates in the following hadronic final states: $K^+\pi^-$, $K^+\pi^-\pi^0$, $K^+\pi^-\pi^0\pi^0$, $K^+\pi^-\pi^-\pi^+$, and $K^+\pi^-\pi^-\pi^+\pi^0$ for neutral tags, and $K^+\pi^-\pi^-$, $K^+\pi^-\pi^-\pi^0$, $K_S^0\pi^-$, $K_S^0\pi^-\pi^0$, $K_S^0\pi^-\pi^+\pi^-$, and $K^+K^-\pi^-$ for charged tags. The tag samples are selected based on two variables calculated in the e^+e^- center-of-mass frame: $\Delta E \equiv E_{\bar{D}} - E_{\text{beam}}$ and $M_{\text{BC}} \equiv \sqrt{E_{\text{beam}}^2 - |\vec{p}_{\bar{D}}|^2}$, where $E_{\bar{D}}$ and $\vec{p}_{\bar{D}}$ are the reconstructed energy and momentum of the \bar{D} candidate, and E_{beam} is the beam energy. If mul-

iple candidates are present per tagged \bar{D} mode, the one with the smallest $|\Delta E|$ is chosen. The yield of each tag mode is obtained from a fit to the M_{BC} distribution following Ref. [13]. We find $(2759.6 \pm 3.7) \times 10^3$ and $(1572.6 \pm 1.5) \times 10^3$ reconstructed neutral and charged tags, respectively.

After a tag is identified, we reconstruct the SL decay $D^{0(+)} \rightarrow \pi^-\pi^{0(+)}e^+\nu_e$ recoiling against the tag by requiring an e^+ candidate and a $\pi^-\pi^{0(+)}$ pair following Ref. [14]. The momentum reconstruction of the e^+ candidate is improved by recovering energy lost due to final-state radiation or bremsstrahlung in the inner detector region. If there are multiple π^0 candidates in an event, the $\gamma\gamma$ combination with its invariant mass closest to the nominal π^0 mass [1] is chosen. To suppress the background to the D^+ signal from the decay of $D^+ \rightarrow K_S^0e^+\nu_e$, $K_S^0 \rightarrow \pi^+\pi^-$, we veto events with a $\pi^+\pi^-$ invariant mass within $\pm 70 \text{ MeV}/c^2$ of the nominal K_S^0 mass [1], which eliminates about 98.3% of such background. The reconstruction of the tag and SL decay candidates must include all charged tracks in the event and satisfy charge conservation. In addition, the maximum energy of extra photon candidates ($E_{\gamma, \text{max}}$), which are not used in the tag and SL decay reconstruction, is required to be less than 0.25 GeV to suppress the background events with extra π^0 .

Finally, we define the variable $U_{\text{miss}} \equiv E_{\text{miss}} - |\vec{P}_{\text{miss}}|$ to identify the SL decay, which peaks at zero for the signal since the neutrino is undetected. Here E_{miss} and \vec{P}_{miss} are the missing energy and momentum of the D meson; they are calculated in the e^+e^- center-of-mass frame by $E_{\text{miss}} = E_{\text{beam}} - E_{\pi\pi} - E_e$ and $\vec{P}_{\text{miss}} = \vec{P}_{\text{SL}} - \vec{P}_{\pi\pi} - \vec{P}_e$, where $E_{\pi\pi}$ and $\vec{P}_{\pi\pi}$ are the energy and momentum of $\pi\pi$ system, \vec{P}_{SL} is the momentum of the SL candidate, which is calculated as $\vec{P}_{\text{SL}} = -\hat{P}_{\text{tag}}\sqrt{E_{\text{beam}}^2 - m_{\bar{D}}^2}$ to improve the U_{miss} resolution. Here \hat{P}_{tag} denotes the unit momentum vector of the \bar{D} tag and $m_{\bar{D}}$ is the nominal \bar{D} mass [1].

The main background contributions are from $D\bar{D}$ decays, while backgrounds from other processes are negligible. For the D^0 decay, the dominant background arises from $D^0 \rightarrow K^*(892)^-e^+\nu_e$, which results in U_{miss} distribution that is predominantly greater than zero. The backgrounds that peak in U_{miss} mostly arise from $D^0 \rightarrow K^-e^+\nu_e$, $K^- \rightarrow \pi^-\pi^0$ and $D^+ \rightarrow K_S^0e^+\nu_e$ decays. For the D^+ decay, the background is dominated by $D^+ \rightarrow \bar{K}^*(892)^0e^+\nu_e$, which peaks near zero and π^0 mass, depending on the $\bar{K}^*(892)^0$ decay mode. With all tag modes combined, we extract the signal yields by performing an unbinned-maximum-likelihood fit to the U_{miss} distribution. The signal is described by the signal MC distribution convolved with a Gaussian function, and the background is modeled by the generic MC distribution convolved with the same Gaussian resolution function. The mean and standard deviation of the Gaussian func-

tion are left free to account for any difference between the U_{miss} resolution in the MC simulation and the data. The fit results are shown in Fig. 1. We obtain signal yields of 1102 ± 45 and 1667 ± 50 for $D^0 \rightarrow \pi^- \pi^0 e^+ \nu_e$ and $D^+ \rightarrow \pi^- \pi^+ e^+ \nu_e$, respectively, where the errors are statistical.

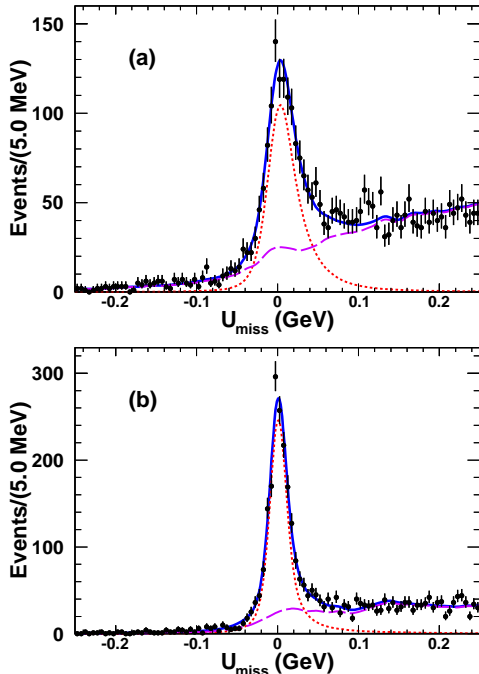


FIG. 1. Fits to the U_{miss} distributions for $D^0 \rightarrow \pi^- \pi^0 e^+ \nu_e$ (a) and $D^+ \rightarrow \pi^- \pi^+ e^+ \nu_e$ (b). The points with error bars are data, and the solid lines are the fits. The short-dashed lines are signals and the long-dashed lines are backgrounds.

To study the $\pi\pi$ system and measure the FF, we require $|U_{\text{miss}}| < 0.06$ GeV to select samples for PWA; this leads to 1498 [2017] events with a background fraction of $(33.28 \pm 0.87)\%$ [$(23.82 \pm 0.69)\%$] in the D^0 [D^+] mode. The differential decay rate for $D^{0(+)} \rightarrow \pi^- \pi^{0(+)} e^+ \nu_e$ depends on five variables [15, 16]: m , the invariant mass of the $\pi\pi$ system; q , the invariant mass of the $e^+ \nu_e$ system; θ_e (θ_π), the angle between the momentum of the e^+ (π^-) in the $e^+ \nu_e$ ($\pi\pi$) rest frame and the momentum of the $e^+ \nu_e$ ($\pi\pi$) system in the D rest frame; and χ , the angle between the normals of the decay planes defined in the D rest frame by the $\pi\pi$ pair and the $e^+ \nu_e$ pair. The sign of χ should be changed when analyzing a \bar{D} candidate in order to maintain CP conservation. In theory, the differential decay rate as a function of these variables is given in Ref. [17]. Neglecting the contributions from the positron mass, it depends on the hadronic FFs as defined in Ref. [16]. For the P -wave contribution, we use the Gounaris-Sakurai (GS) function [18] to describe ρ^- and ρ^0 ; the $\rho^0 - \omega$ interference is taken into account by

the form $R_{\rho^0-\omega}(m) = \text{GS}_{\rho^0}(m) \times [1 + a_\omega e^{i\phi_\omega} \text{RBW}_\omega(m)]$, where RBW is a relativistic Breit-Wigner function with a constant width [19]. A Blatt-Weisskopf damping factor (r_{BW}) related to the meson radii is included in the decay amplitude. The q^2 dependence of the total FFs are parametrized in terms of one vector FF [$V(q^2)$] and two axial vector FFs [$A_{1,2}(q^2)$] that are assumed to be dominated by a single pole: $V(q^2) = \frac{V(0)}{1 - q^2/m_V^2}$, $A_{1,2}(q^2) = \frac{A_{1,2}(0)}{1 - q^2/m_A^2}$. Here m_V and m_A are the pole masses and fixed to $m_{D^*(1-)} \simeq 2.01$ GeV/ c^2 and $m_{D^*(1+)} \simeq 2.42$ GeV/ c^2 [1] in the fit, respectively. At $q^2 = 0$, the FF ratios, $r_V = \frac{V(0)}{A_1(0)}$ and $r_2 = \frac{A_2(0)}{A_1(0)}$, are determined from the fit to the differential decay rate. These ansätze are adequate according to the fit results shown in Figs. 2 (b) and 2 (g). The S -wave contribution, characterized by the FF \mathcal{F}_{10} , is parametrized, assuming only $f_0(500)$ production, as

$$\mathcal{F}_{10} = p_{\pi\pi} m_D \frac{a_S e^{i\phi_S} \mathcal{A}_S(m)}{1 - \frac{q^2}{m_A^2}}, \quad (1)$$

where $p_{\pi\pi}$ is the magnitude of the three-momentum of the $\pi\pi$ system in the D rest frame. Here the term $\mathcal{A}_S(m)$ corresponds to the mass-dependent S -wave amplitude modeled by the fixed resonant line shape described in Ref. [20]; the parameters a_S and ϕ_S are the magnitude and phase of $\mathcal{A}_S(m)$ relative to $\text{GS}_{\rho^0}(m)$.

We perform the PWA using an unbinned-maximum-likelihood fit. The negative log likelihood $-\ln \mathcal{L}$ is defined as

$$-\sum_{i=1}^N \ln \left((1 - f_b) \frac{\omega(\xi_i, \eta)}{\int d\xi_i \omega(\xi_i, \eta) \epsilon(\xi_i)} + f_b \frac{B_\epsilon(\xi_i)}{\int d\xi_i B_\epsilon(\xi_i) \epsilon(\xi_i)} \right), \quad (2)$$

where ξ_i denotes the five kinematic variables characterizing the i th event of N and η denotes the fit parameters; $\omega(\xi_i, \eta)$ is the decay intensity, and $B_\epsilon(\xi_i)$ is defined to be the background distribution corrected by the acceptance function $\epsilon(\xi_i)$ [21]. The background shape is parametrized using the generic MC and its fraction f_b is fixed according to the result of the U_{miss} fit. We model the background with a nonparametric function class RooNDKeysPdf [22] that uses an adaptive kernel-estimation algorithm [23]. The normalization integral in the denominator is determined using a MC technique [13].

A simultaneous PWA fit is performed on both isospin-conjugate modes. The structure of the $\pi\pi$ system is only the ρ^- in the D^0 mode and is dominated by the ρ^0 , with a small fraction of ω , in the D^+ mode. In the fit, the masses and widths of ρ and ω are fixed to those reported in Ref. [1]. We also consider other possible components in the D^+ mode, especially a $\pi^+ \pi^-$ S -wave contribu-

tion from the $f_0(500)$. We find that the $\cos\theta_\pi$ distribution of the fit can agree with data only after considering the S -wave contribution. The statistical significance of the $f_0(500)$ is determined to be more than 10σ from the change of $-2\ln\mathcal{L}$ in the PWA fits with and without this component, taking into account the change of the number of degrees of freedom. The projections of the five kinematic variables for the data are shown in Fig. 2. The difference of the $\cos\theta_\pi$ distribution between two modes is due to the $\pi^+\pi^-$ S -wave interference contribution in D^+ decays. Based on this nominal solu-

tion, we obtain the fractions of the different components: $f_{f_0(500)} = (25.7 \pm 1.6 \pm 1.1)\%$, $f_{\rho^0} = (76.0 \pm 1.7 \pm 1.1)\%$ and $f_\omega = (1.28 \pm 0.41 \pm 0.15)\%$, as well as the FF ratios $r_V = 1.695 \pm 0.083 \pm 0.051$ and $r_2 = 0.845 \pm 0.056 \pm 0.039$, with a correlation coefficient $\rho_{r_V, r_2} = -0.206$, where the first and second uncertainties are statistical and systematic, respectively. To calculate the fractions and estimate the corresponding statistical uncertainties, we employ the same method described in Ref. [24]. As a cross check, we perform fits to the two modes separately, and the results are consistent with the simultaneous fit.

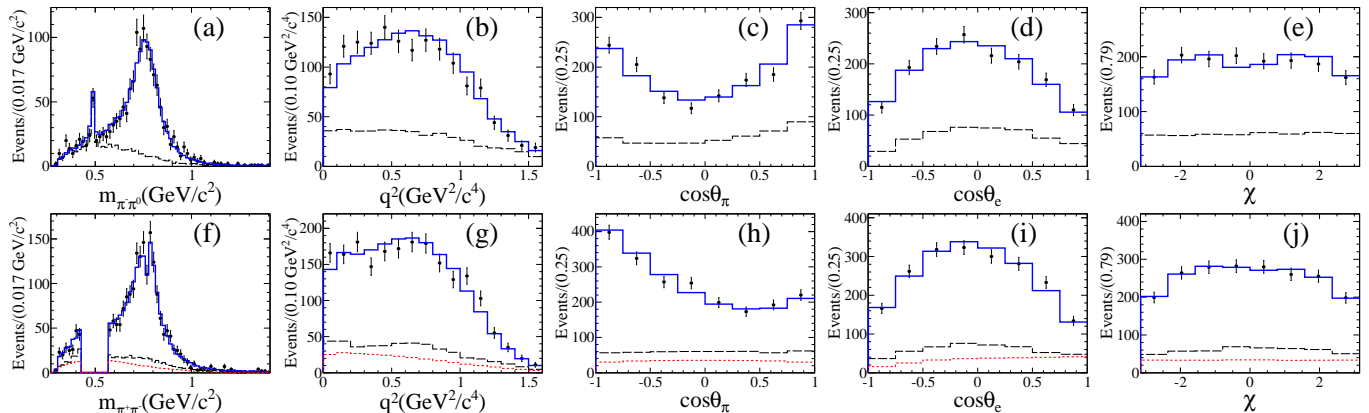


FIG. 2. Projections of the data and simultaneous PWA fit onto the five kinematic variables for $D^0 \rightarrow \pi^-\pi^0 e^+\nu_e$ (top) and $D^+ \rightarrow \pi^-\pi^+ e^+\nu_e$ (bottom) channels. The dots with error bars are data, the solid lines are the fits, the dashed lines show the MC simulated backgrounds, and the short-dashed lines in (f)-(j) show the component of $D^+ \rightarrow f_0(500)e^+\nu_e$.

Replacing the $f_0(500)$ component with a phase-space S -wave amplitude worsens the $-\ln\mathcal{L}$ by 40.3. If the phase-space S -wave amplitude is added to the nominal solution on top of the $f_0(500)$ component, its statistical significance is only about 1σ , so this contribution is neglected. In addition, a possible $f_0(980)$ component contributing to the \mathcal{F}_{10} term is studied by adding it to the nominal solution, where $f_0(980)$ is parametrized by the Flatté formula with its parameters fixed to the BESII measurements [25]. The significance of this component is less than 2σ . By scanning the BF of the $f_0(980)$ component in the physical region, we obtain an upper limit at the 90% confidence level (CL), which is listed in Table I. To take the systematic uncertainty into account, the likelihood is convolved with a Gaussian function with a resolution equal to the systematic uncertainty.

We calculate the absolute BFs of both modes with the same method as described in Ref. [13]. For the D^0 mode, the only significant contribution observed is $D^0 \rightarrow \rho^- e^+\nu_e$. For the D^+ mode, the absolute BFs of the different components are derived from $\mathcal{B}(D^+ \rightarrow \pi^-\pi^+ e^+\nu_e) \times f_i$, where i denotes the different components of the $\pi\pi$ system: $f_0(500)$, ρ^0 , and ω , and f_i denotes the fraction obtained via the PWA. The BFs of $\pi^0 \rightarrow \gamma\gamma$ and $\omega \rightarrow \pi^+\pi^-$ [1] have been included in the calculation. All the results are summarized in Table I.

TABLE I. Measured absolute BFs and upper limit of the BF at 90% CL. The first (second) uncertainties are statistical (systematic).

Signal mode	this analysis ($\times 10^{-3}$)
$D^0 \rightarrow \pi^-\pi^0 e^+\nu_e$	$1.445 \pm 0.058 \pm 0.039$
$D^0 \rightarrow \rho^- e^+\nu_e$	$1.445 \pm 0.058 \pm 0.039$
$D^+ \rightarrow \pi^-\pi^+ e^+\nu_e$	$2.449 \pm 0.074 \pm 0.073$
$D^+ \rightarrow \rho^0 e^+\nu_e$	$1.860 \pm 0.070 \pm 0.061$
$D^+ \rightarrow \omega e^+\nu_e$	$2.05 \pm 0.66 \pm 0.30$
$D^+ \rightarrow f_0(500)e^+\nu_e, f_0(500) \rightarrow \pi^+\pi^-$	$0.630 \pm 0.043 \pm 0.032$
$D^+ \rightarrow f_0(980)e^+\nu_e, f_0(980) \rightarrow \pi^+\pi^-$	< 0.028

For the BF measurements, most systematic uncertainties related to the tag side are canceled when the double-tag technique is employed; therefore, systematic uncertainties arise mainly from the reconstruction of the SL decay. The systematic uncertainty associated with the tag yield for the D^0 (D^+) signal is estimated to be 0.2% (0.4%) by varying the M_{BC} fit range. The uncertainties related to the π^\pm tracking efficiency, π^\pm particle identification (PID) efficiency and π^0 reconstruction efficiency are estimated to be 0.8% (1.2%), 0.2% (0.3%), and 0.6%, respectively, by studying the doubly tagged $D\bar{D}$ hadronic decay samples. Using a sample of radiative Bhabha events, the uncertainty of the e^\pm PID ef-

efficiency is estimated to be 0.5% for both modes. The uncertainty from the e^\pm energy recovery is estimated to be 0.4% (0.7%) by comparing to the BFs obtained without recovery. The uncertainty from the K_S^0 veto is estimated to be 1.8% by varying the size of the veto window. The fully reconstructed $D\bar{D}$ hadronic decays are used to show that the uncertainty due to the $E_{\gamma,\max}$ requirement is negligible. We estimate the uncertainty in the signal yield of the U_{miss} fit to be 1.5% (0.5%) by varying the fitting range. The uncertainty related to the modeling of the background shape is estimated to be 1.5% (1.4%) by changing the BFs of the dominant background channels by $\pm 1\sigma$, and σ is the uncertainty reported in Ref. [1]. We estimate the uncertainty due to the PWA model of the signal to be 0.3% (0.9%) by varying the parameters of the nominal solution by their statistical uncertainty. These estimates are added in quadrature to obtain the total systematic uncertainty of 2.5% (3.0%) for D^0 (D^+) mode.

The following sources of systematic uncertainties, as summarized in Table II, have been considered in the PWA procedure. The uncertainty related to variations to the fit are estimated by taking the difference between the alternative fit and the nominal fit. The uncertainty from the modeling of the background shape is assigned as for the BF measurement. The uncertainty due to the fixed background fraction f_b is estimated by changing by $\pm 1\sigma$ of its statistical error. The parameter of r_{BW} is set to 3.0 GeV^{-1} in the nominal fit; the uncertainty related to this imperfect knowledge is estimated by varying the value within $2.0 - 4.0 \text{ GeV}^{-1}$. We vary m_V and m_A by $\pm 100 \text{ MeV}/c^2$ to estimate the uncertainties associated with the pole mass assumption. The uncertainty from the ρ or ω line shape is estimated by varying the mass and width of ρ or ω by $\pm 1\sigma$ error [1]. The systematic uncertainty of the $f_0(500)$ modeling is considered by replacing with a conventional RBW function with the mass and width fixed to the BESII measurements [26]. The possible bias due to the fit procedure is studied with the same method described in Ref. [24]. The mean bias is taken as a corresponding systematic uncertainty.

TABLE II. Absolute systematic uncertainties on the FF ratios and the fractions of different components in D^+ decays.

Source	r_V	r_2	$f_{f_0(500)}$ (%)	f_{ρ^0} (%)	f_ω (%)
Background shape	0.003	0.003	0.06	0.06	0.009
Background fraction	0.008	0.021	0.32	0.25	0.060
r_{BW}	0.024	0.026	0.56	0.56	0.059
m_V	0.035	0.001	0.02	0.02	0.004
m_A	0.025	0.020	0.06	0.04	0.013
ρ line shape	0.002	0.003	0.05	0.02	0.034
ω line shape	0.0002	0.0002	0.02	0.09	0.008
$f_0(500)$ modeling	0.012	0.005	0.83	0.88	0.038
Fit procedure	0.003	0.003	0.18	0.27	0.086
Total	0.051	0.039	1.07	1.11	0.15

In summary, the SL decays $D^0 \rightarrow \pi^-\pi^0 e^+\nu_e$ and $D^+ \rightarrow \pi^-\pi^+ e^+\nu_e$ are studied using a data sample corresponding to an integrated luminosity of 2.93 fb^{-1} collected with the BESIII detector at $\sqrt{s} = 3.773 \text{ GeV}$. We measure the FF in $D \rightarrow \rho e^+\nu_e$ via a simultaneous PWA fit to both decay channels, and improve the absolute BFs for these decays. The FF measurements are consistent with the only measurement [8] but with improved precision. These measurements are compatible with the theoretical calculations [6, 7] that have much larger uncertainty than experimental results. They can also aid the determination of V_{ub} via a double-ratio technique [27]. The BF results are consistent with isospin invariance: $\frac{\Gamma(D^0 \rightarrow \rho^- e^+\nu_e)}{2\Gamma(D^+ \rightarrow \rho^0 e^+\nu_e)} = 0.985 \pm 0.054 \pm 0.043$. The BFs of different components contributing to the $D^+ \rightarrow \pi^-\pi^+ e^+\nu_e$ decay are also obtained. The hadronic system in this decay is dominated by the P wave, which is mostly a ρ^0 contribution along with a much smaller one from the ω . Additionally, the S -wave process $D^+ \rightarrow f_0(500)e^+\nu_e$ is observed for the first time with a relative contribution of $(25.7 \pm 1.6 \pm 1.1)\%$. This is compatible with the theoretical predictions reported in Refs. [4, 5]. The process $D^+ \rightarrow f_0(980)e^+\nu_e$ is not significant and an upper limit on its BF is set at the 90% CL.

In the SU(3) symmetry limit, Ref. [28] proposed a model-independent way to distinguish the two different descriptions of the scalar mesons using a ratio $R = \frac{\mathcal{B}(D^+ \rightarrow f_0(980)e^+\nu_e) + \mathcal{B}(D^+ \rightarrow f_0(500)e^+\nu_e)}{\mathcal{B}(D^+ \rightarrow a_0(980)^0 e^+\nu_e)}$, which is predicted to be 1.0 ± 0.3 for the two-quark description and 3.0 ± 0.9 for the tetraquark description. We obtain $R > 2.7$ at the 90% CL by using $\mathcal{B}(f_0(500) \rightarrow \pi^+\pi^-) = 67\%$, $\mathcal{B}(a_0(980)^0 \rightarrow \pi^0\eta) = 85\%$ [1] and the BESIII measurement [29] for $D^+ \rightarrow a_0(980)^0 e^+\nu_e$. Here, we neglect the $f_0(980)$ component and assume that the dominant decays are $\pi\pi$ for $f_0(500)$, and $\pi\eta$ and $K\bar{K}$ for $a_0(980)^0$. Our result favors the SU(3) nonet tetraquark description of the $f_0(500)$, $f_0(980)$ and $a_0(980)$.

The BESIII collaboration thanks the staff of BEPCII and the IHEP computing center for their strong support. This work is supported in part by National Key Basic Research Program of China under Contract No. 2015CB856700; National Natural Science Foundation of China (NSFC) under Contracts Nos. 11075174, 1121092, 11405046, 11475185, 11575091, 11625523, 11635010, 11775246; the Chinese Academy of Sciences (CAS) Large-Scale Scientific Facility Program; the CAS Center for Excellence in Particle Physics (CCEPP); Joint Large-Scale Scientific Facility Funds of the NSFC and CAS under Contracts Nos. U1332201, U1532257, U1532258; CAS under Contracts Nos. KJCX2-YW-N29, KJCX2-YW-N45, QYZDJ-SSW-SLH003; 100 Talents Program of CAS; National 1000 Talents Program of China; INPAC and Shanghai Key Laboratory for Particle Physics and Cosmology; German Research Foundation DFG under Contracts Nos. Collaborative Re-

search Center CRC 1044, FOR 2359; Istituto Nazionale di Fisica Nucleare, Italy; Joint Large-Scale Scientific Facility Funds of the NSFC and CAS; Koninklijke Nederlandse Akademie van Wetenschappen (KNAW) under Contract No. 530-4CDP03; Ministry of Development of Turkey under Contract No. DPT2006K-120470; National Natural Science Foundation of China (NSFC) under Contract No. 11505010; National Science and Technology fund; The Swedish Research Council; U. S. Department of Energy under Contracts Nos. DE-FG02-05ER41374, DE-SC-0010118, DE-SC-0010504, DE-SC-0012069; University of Groningen (RuG) and the Helmholtzzentrum fuer Schwerionenforschung GmbH (GSI), Darmstadt; WCU Program of National Research Foundation of Korea under Contract No. R32-2008-000-10155-0.

-
- [1] C. Patrignani *et al.* (Particle Data Group), *Chin. Phys. C* **40**, 100001 (2016).
- [2] R. L. Jaffe, *Phys. Rev. D* **15**, 267 (1977); A. H. Fariborz, R. Jora, and J. Schechter, *Phys. Rev. D* **79**, 074014 (2009); G. Mennessier, S. Narison, and X. G. Wang, *Phys. Lett. B* **696**, 40 (2011); N. N. Achasov and A. V. Kiselev, *Phys. Rev. D* **86**, 114010 (2012); **83**, 054008 (2011); S. Weinberg, *Phys. Rev. Lett.* **110**, 261601 (2013).
- [3] E. van Beveren, T. A. Rijken, K. Metzger, C. Dullemond, G. Rupp, and J. E. Ribeiro, *Z. Phys. C* **30**, 615 (1986); E. van Beveren, D. V. Bugg, F. Kleefeld, and G. Rupp, *Phys. Lett. B* **641**, 265 (2006); J. R. Pelaez, *Phys. Rev. Lett.* **92**, 102001 (2004); M. Wakayama, T. Kunihiro, S. Muroya, A. Nakamura, C. Nonaka, M. Sekiguchi, and H. Wada, *Phys. Rev. D* **91**, 094508 (2015).
- [4] T. Sekihara and E. Oset, *Phys. Rev. D* **92**, 054038 (2015).
- [5] Y. J. Shi, W. Wang, and S. Zhao, *Eur. Phys. J. C* **77**, 452 (2017).
- [6] J. M. Flynn and C. T. Sachrajda, *Adv. Ser. Direct. High Energy Phys.* **15**, 402 (1998).
- [7] P. Ball, *Phys. Rev. D* **48**, 3190 (1993).
- [8] S. Dobbs *et al.* (CLEO Collaboration), *Phys. Rev. Lett.* **110**, 131802 (2013).
- [9] J. Adler *et al.* (MARK-III Collaboration), *Phys. Rev. Lett.* **62**, 1821 (1989).
- [10] M. Ablikim *et al.* (BESIII Collaboration), *Chin. Phys. C* **37**, 123001 (2013).
- [11] M. Ablikim *et al.* (BESIII Collaboration), *Phys. Lett. B* **753**, 629 (2016).
- [12] M. Ablikim *et al.* (BESIII Collaboration), *Nucl. Instrum. Meth. A* **614**, 345 (2010).
- [13] M. Ablikim *et al.* (BESIII Collaboration), *Phys. Rev. D* **94**, 032001 (2016).
- [14] M. Ablikim *et al.* (BESIII Collaboration), *Phys. Rev. D* **92**, 071101(R) (2015).
- [15] N. Cabibbo and A. Maksymowicz, *Phys. Rev.* **137**, B438 (1965).
- [16] P. del Amo Sanchez *et al.* (BABAR Collaboration), *Phys. Rev. D* **83**, 072001 (2011).
- [17] C. L. Y. Lee, M. Lu, and M. B. Wise, *Phys. Rev. D* **46**, 5040 (1992).
- [18] G. J. Gounaris and J. J. Sakurai, *Phys. Rev. Lett.* **21**, 244 (1968).
- [19] R. R. Akhmetshin *et al.*, (CMD-2 collaboration) *Phys. Lett. B* **527**, 161 (2002).
- [20] D. V. Bugg, *J. Phys. G* **34**, 151 (2007).
- [21] M. Artuso *et al.* (CLEO Collaboration), *Phys. Rev. D* **85**, 122002 (2012).
- [22] W. Verkerke and D. P. Kirkby, *RooFit Users Manual v2.91*.
- [23] K. Cranmer, *Comput. Phys. Commun.* **136**, 198 (2001).
- [24] M. Ablikim *et al.* (BESIII Collaboration), *Phys. Rev. D* **95**, 072010 (2017).
- [25] M. Ablikim *et al.* (BESII Collaboration), *Phys. Lett. B* **607**, 243253 (2005).
- [26] M. Ablikim *et al.* (BESII Collaboration), *Phys. Lett. B* **598**, 149 (2004).
- [27] B. Grinstein and D. Pirjol, *Phys. Rev. D* **70**, 114005 (2004).
- [28] W. Wang and C. D. Lu, *Phys. Rev. D* **82**, 034016 (2010).
- [29] M. Ablikim *et al.* (BESIII Collaboration), *Phys. Rev. Lett.* **121**, 081802 (2018).